KKU Res.j. 2015; 20(4) : 393-404
http://resjournal.kku.ac.th

Heat Transfer and Fluid Flow Behavior of Air in Square Duct Heat Exchanger Inserted with V-downstream Winglet Turbulators

Suriya Chokphoemphun[1], Sanhawat Thongdaeng[1] and Pongjet Promvonge[2]*

[1]*Major of Mechanical Engineering, Faculty of Industry and Technology, Rajamangala University of Technology Isan Sakonnakhon Campus, Sakonnakhon, Thailand*
[2]*Department of Mechanical Engineering, Faculty of Engineering, King Mongkut's Institute of Technology Ladkrabang, Bangkok, Thailand*
[*]*Correspondent author: chok_suriya_@hotmail.com*

Abstract

This work present the experimental investigation on heat transfer enhancement and thermal performance in a square-duct heat exchanger inserted with 45º V-downstream winglet turbulator is carried out by varying velocity of air in the turbulent regime for Reynolds numbers (Re) ranging from 4000 to 26,000 in the test section with a constant wall heat flux condition. Influents of four different pitch lengths; P=22.5, 33.75, 45 and 90 mm (P_R=P/H=0.5, 0.75, 1 and 2) and three different winglet heights, e=6.75, 9 and 11.25 mm (B_R=e/H=0.15, 0.2 and 0.25) were inserted diagonally and placed in the core flow area into the test duct on heat transfer rates in the term of Nusselt number (Nu), pressure loss in form of friction factor (*f*) and thermal performance (η). It was found that the 45º V-downstream winglet is provided the Nu and *f* higher than the smooth surface around 6.0 to 8.7 times and 37 to 170 times, respectively depending upon operating conditions while the thermal performance are about 1.50–2.06. The maximum thermal performance for using 45º V-downstream winglet turbulator is 2.06 at Re=4100, B_R=0.2 and P_R=1.0 in this experiment.

Keywords : *V-downstream winglet, square-duct heat exchanger, thermal performance*

1. Introduction

Many researchers have been carried out to study the effect of geometry of turbulent promotor/turbulator for enhancing the heat transfer rate and improving the thermal performance enhancement factor as seen in the Ref (1–2). The main aim of investigation is to make more compact or high performance heat exchangers, possibly their cost or to reduce the pumping power required for a given heat transfer process, which can result in a saving of investment or operating costs. In general, heat transfer enhancements technics can be classifieds into three methods: active, passive and combine method. Within the passive category, insertion of turbulator device is one of the most promising techniques because this method can be easily employed in an existing heat exchanger without requiring an additional extra power source.

Varun et al. (3) studied experimentally the heat transfer and friction characteristics by using a combination of inclined ribs on the absorber plate of a solar air heater. Results show that the roughened collector with absorber plate having relative roughness pitch of 8 gives the best performance. The heat transfer and fluid flow characteristics in a duct heat exchanger fitted with curved trapezoidal, rectangular, trapezoidal and delta winglets were experimentally investigated by Zhou and Ye (4). Influent of combined turbulator (ribs and winglet) on convective heat transfer and friction loss behaviors for turbulent airflow through a constant heat fluxed channel were presented by Promvonge et al. (5). Won and Ligrani (6) carried out experimentally a comparison of heat transfer characteristics of channels with 45° parallel and crossed ribs and found that the 45° parallel ribs perform better than the 45° crossed ribs. Promvonge et al. (7, 8) presented the numerically study the thermal characteristics in a square channel with 30° and 45° angled baffles on two opposite walls and compared with the 90° transverse baffles.

Chokphoemphun et al. (9) presents the effect of V-Shape winglet vortex generators with a different attack angle, winglet-height and winglet pitch length were inserted placed in the core flow area into the test tube on thermal performance enhancement of a uniform wall heat-fluxed tube heat exchanger in turbulent regime. The influence of 30° incline winglet vortex generators with four different winglet pitch ratios and three blockage ratios inserted in the core flow area on heat transfer rate and pressure loss of tube heat exchanger was reported by Chokphoemphun et al. (10).

Most of the investigations, cited above, have focused on thermal performance for various blockage and pitch ratios for baffles/ribs/winlets that placing on surfaces of duct or channels and rarely been found to be inserted it on the core flow of the tube heat exchangers. In the present work, the 45° V-downstream winglet turbulator are mounted periodically on double-sides of a straight tape inserted diagonally and placed in duct heat exchanger are conducted with the main aim to examine the heat transfer and fluid flow behaviors.

2. Data reduction

2.1 Nusselt number

The heat transfer is presented in a term of the average Nusselt number as seen in the Ref (11) which can be obtained by.

$$Nu = \frac{hD_h}{k} \tag{1}$$

Where h is the average heat transfer coefficient, D_h is the duct hydraulic diameter and k is the thermal conductivity of air.

The average heat transfer coefficient will be evaluated from the experimental data via the following equations:

$$h = \dot{m}C_{p,a}\left(T_o - T_i\right) / A\left(\tilde{T}_w - T_b\right) \tag{2}$$

Where $\dot{m}$ is mass flow rate, $C_{p,a}$ is specific heat of air, T_i and T_o is the inlet and outlet temperature of air, $\tilde{T}_w$ is average wall temperature were calculated from 28 points of surface temperatures, T_b is the bulk temperature and A is heat transfer surface area.

The Nusselt number ratio is defined as the ratio of the Nusselt number of an augmented surface to that of a smooth surface (subscribe, 0).

$$Nu \text{ ratio} = \frac{Nu}{Nu_0} \quad (3)$$

2.2 Friction factor

The friction factor (f) computed by pressure drop across the test section length (L) as seen in the Ref (12) is written as

$$f = \frac{2}{(L/D_h)} \frac{\Delta P}{\rho U^2} \quad (4)$$

Where ΔP is the pressure drop, L is the length of test section, D_h is the hydraulic diameter of square duct, ρ is the air density and U is the mean air velocity.

The friction factor ratio is defined as the ratio of the friction factor of an augmented surface to that of a smooth surface (subscribe, 0).

$$f \text{ ratio} = \frac{f}{f_0} \quad (5)$$

2.3 Thermal performance

The thermal performance factor defined as the relationship of the Nusselt number ratio and friction factor ratio at the same level of pumping power as seen in the Ref (13) and can be expressed as follows.

$$\eta = \left(\frac{Nu}{Nu_0}\right)\left(\frac{f}{f_0}\right)^{-1/3} \quad (6)$$

3. Experimental setup and Winglet Turbulator

The detail of the experimental apparatus used in the present work is shown schematically in Figure 1. In the apparatus, the inlet bulk air at 25 °C from a 1.45 kW blower was directed through an orifice flow-meter, settling tank and passed to the test square-duct. The airflow rate was measured by the orifice-meter, built according to ASME standard (14) and calibrated by using a hot-wire anemometer to measure flow velocities across the test duct. Manometric fluid was used in an inclined manometer with specific gravity (SG) of 0.826 to ensure reasonably accurate measurement of pressure drop across the orifice. The desired volumetric airflow rate from the blower was obtained by controlling the motor speed of the blower through an inverter. The 3 mm thick aluminum square-duct having a cross section (H×H) of 45×45 mm^2 and overall length of 3000 mm and was divided into two sections: a clam section of 2000 mm and a test section (L) of 1000 mm. The AC power supply was the source of power for the plate-type heater used for heating all walls of the test section and maintain a uniform surface heat flux and the outer surface of the test section was well insulated to minimize heat loss to surroundings. The temperature distributions along the outer surface of the test section were measured by 28 type-K thermocouples (11-points on upper wall, 11-points on side walls and 6-points on lower wall) while the inlet and outlet air temperatures at upstream and downstream of the test duct were measured by 2 RTD PT-100. All of the temperature readings from the measurement system were consistently recorded using a data logger. The pressure drop across the test section was measured by two static pressure taps, mounted on the upper wall at upstream and downstream positions of the test section and observed measurable value from a digital manometer. Reynolds numbers for the air flowing through the test section were controlled in the range of 4000 to 26,000.

To quantify the uncertainties of measurements, the reduced data obtained experimentally were determined. The uncertainty in the data calculation was based on ref. (15). The maximum uncertainties of non-dimensional parameters were ±5% for Reynolds number, ±7% for Nusselt number and ±8% for friction. The uncertainty in the axial velocity measurement was estimated to be less than ±5%, and pressure has a corresponding estimated uncertainty of±5%, whereas the uncertainty in temperature measurement at the duct wall was about ±0.5%.

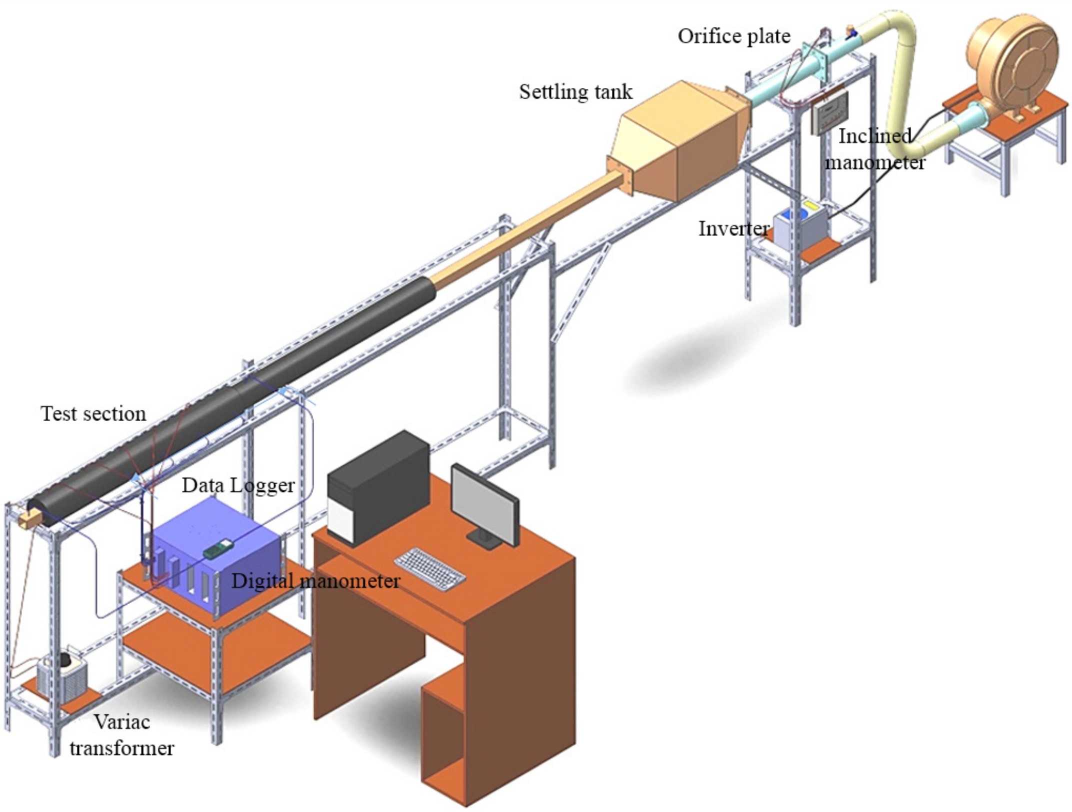

Figure 1. Schematic diagram of experimental apparatus.

A detail of the test duct inserted with 45º V-downstream winglet turbulator is depicted in Figure. 2. All winglet made of aluminum strip were 0.3 mm thick. As seen in figure, the V-downstream winglet elements are mounted on the core flow with attack angle of 45° with respect to the main flow direction on both side of straight tape. The V-downstream winglet were inserted in the test duct with four different pitch lengths; P=22.5, 33.75, 45 and 90 mm (P_R=P/H=0.5, 0.75, 1 and 2) and three different winglet heights, e=6.75, 9 and 11.25 mm (B_R=e/H=0.15, 0.2 and 0.25).

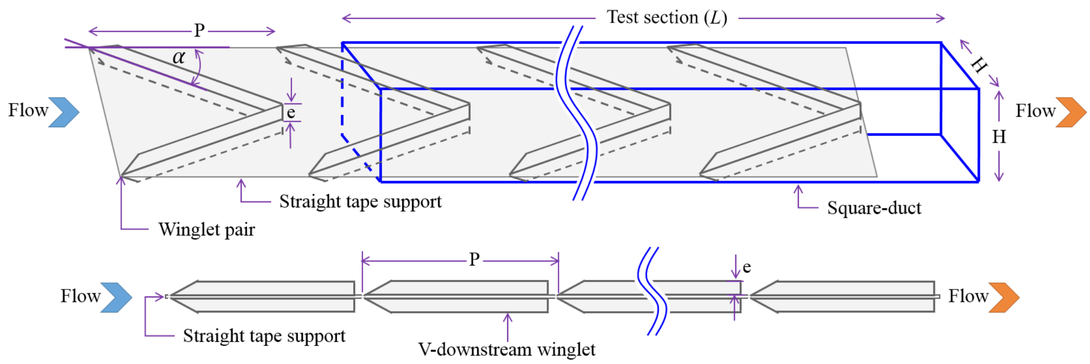

Figure 2. V-downstream winglet with straight tape inserted into test section.

4. Results and Discussion

4.1 Validation of smooth tube

The present experimental results on the heat transfer and friction characteristics in a smooth wall duct were first validated in terms of Nusselt number (Nu) and friction factor (*f*), respectively. The Nu obtained from the present smooth duct was compared with that from correlations of Dittus-Boelter and Gnielinski while the *f* was compared with data from correlations of Blasius and Petukhov found in the open literature (16).

Correlation of Dittus and Boelter

$$\mathrm{Nu} = 0.023\,\mathrm{Re}^{0.8}\,\mathrm{Pr}^{0.4} \tag{7}$$

Correlation of Gnielinski

$$\mathrm{Nu} = \frac{(f/8)(\mathrm{Re}-1000)\,\mathrm{Pr}}{1+12.7(f/8)^{1/2}(\mathrm{Pr}^{2/3}-1)} \tag{8}$$

Correlation of Blasius

$$f = 0.316\,\mathrm{Re}^{-0.25} \tag{9}$$

Correlation of Petukhov

$$f = (0.79\ln \mathrm{Re} - 1.64)^{-2} \tag{10}$$

Figure 3 shows a comparison of the Nu and *f* obtained from the present work with those from correlations from previous works available for steady state flow conditions for smooth duct. As shown in the figure, the present results are in good agreement with those from available correlations within ±4% and ±5% in comparison with Dittus-Boelter and Gnielinski correlations, respectively, for Nu and ±3% and ±5% in comparison with both Blasius and Petukhov for *f*.

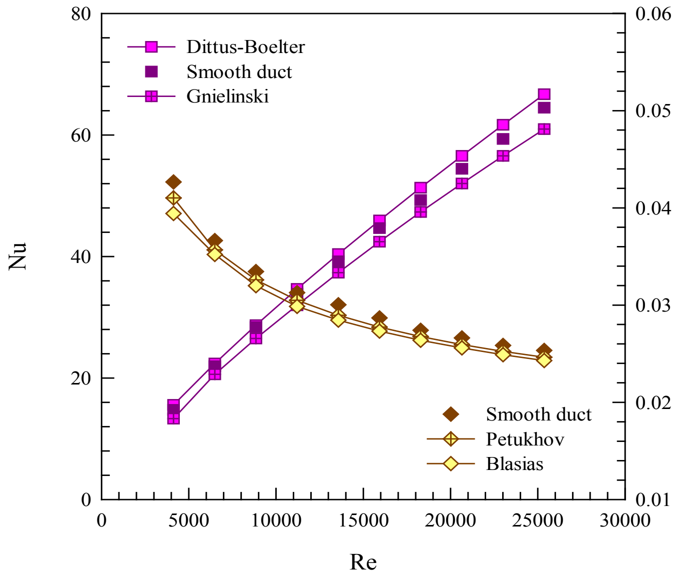

Figure 3. Verification of Nusselt number and friction factor for smooth duct.

4.2 Effect of V-downstream winglet on heat transfer

The relationships between heat transfer (Nu) and Reynolds numbers (Re) of the square-duct heat exchanger inserted with 45° V-downstream winglet are demonstrated in Figure 4. According to the figure, the heat transfer enhancement values of the inserted duct are found to be better than that the smooth duct. This is due to the interruption of the flow by the turbulators which results in the destruction of thermal boundary layer near the duct wall. The Nu increases with the rise of Re and the B_R and with the decreasing of the P_R.

The Nusselt number ratio (Nu/Nu_0) plotted against the Re values is displayed in Figure 5. The figure present, the Nu/Nu_0 tends to slightly decrease with the rise of Re for all case study. Under the present experimental conditions, the increases in heat transfer over the smooth duct for using the V-downstream winglet with P_R of 0.5, 0.75, 1 and 2 are approximately 7.41–7.52, 7.11–7.28, 6.68–6.77 and 6.00–6.09 times for B_R=0.15, 8.34–8.44, 8.16–8.24, 7.87–7.97 and 7.02–7.17 times for B_R=0.2 and 8.53–8.65, 8.40–8.51, 8.20–8.33 and 7.39–7.48 times for B_R=0.25. The mean Nu values for B_R=0.15, 0.2 and 0.25 are about 7.41–7.52, 8.34–8.44 and 8.53–8.65 times for P_R=0.5, 7.11–7.28, 8.16–8.24 and 8.40–8.51 times for P_R=0.75, 6.68–6.77, 7.87–7.97 and 8.20–8.33 times for P_R=1 and 6.00–6.09, 7.02–7.17 and 7.39–7.48 times for P_R=2 over the smooth duct.

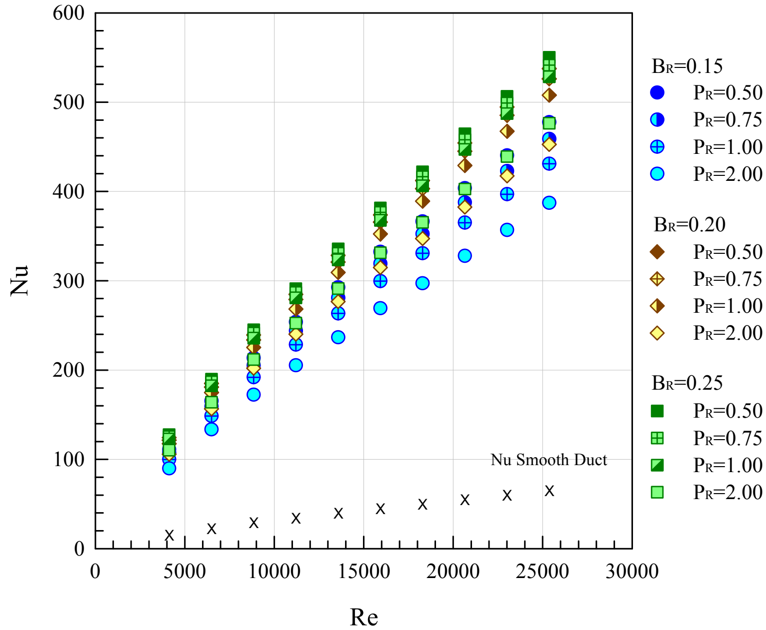

Figure 4. Demonstrates the variation of the Nusselt number with the Reynolds numbers.

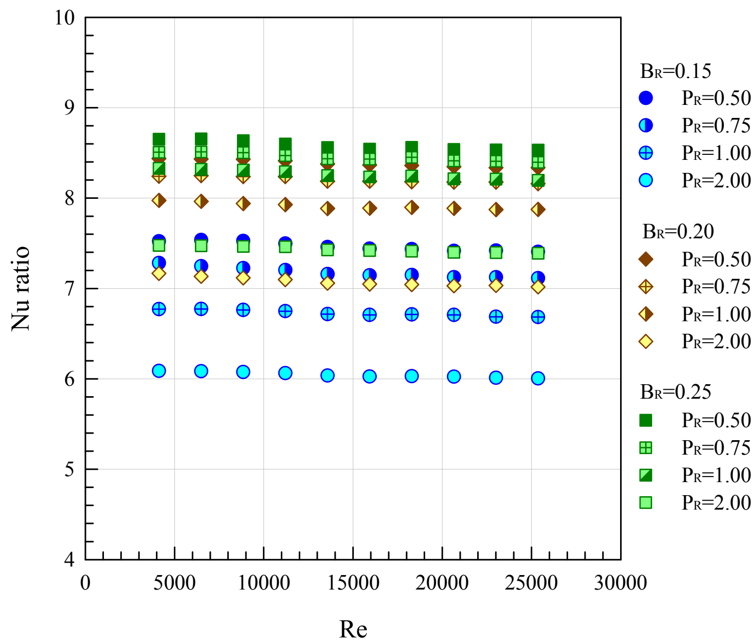

Figure 5. Demonstrates the variation of the Nusselt number ratio with the Reynolds numbers.

4.3 Effect of V-downstream winglet on friction factor

Figure 6 shows the relation between the friction factor (*f*) and the Reynolds number (Re) obtained from the 45° V-downstream winglet inserted. It is observed that the *f* tends to slightly decrease with raising the Re. The V-downstream winglet gives rise to the *f* values higher than that of the smooth duct. The *f* decreases with the rise of the PR and increases with the increasing of the BR. The higher friction loss mainly comes from the increased surface area and higher swirl intensity.

The variation of the friction factor ratio (f/f_0) with the Re values are presented in Figure 7. It is observed that the f/f_0 tends to increase with raising the Re for all case study. Under the present experimental conditions, the increases in f for using the V-downstream winglet with PR of 0.5, 0.75, 1 and 2 are approximately 59–99, 52–85, 40–64 and 37–61 times for BR=0.15, 79–133, 70–118, 58–95 and 54–88 times for BR=0.2 and 101–169, 94–157, 78–129 and 72–120 times for BR=0.25. The mean f values for BR=0.15, 0.2 and 0.25 are about 59–99, 79–133 and 101–169 times for PR=0.5, 52–85, 70–118 and 94–157 times for PR=0.75, 40–64, 58–95 and 78–129 times for PR=1 and 37–61, 54–88 and 72–120 times for PR=2 over the smooth duct.

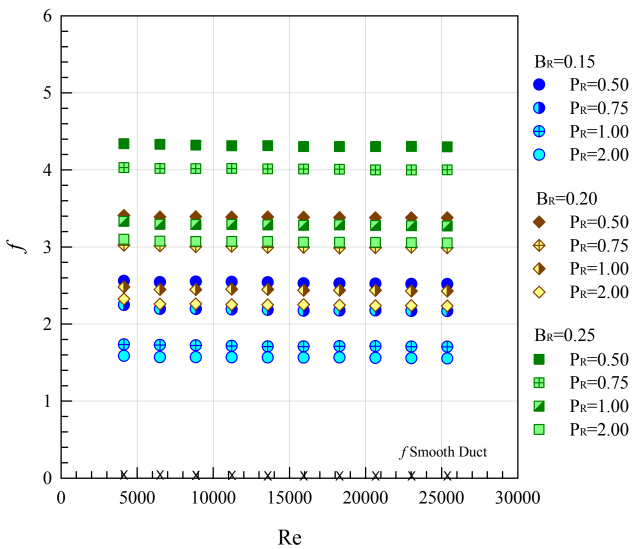

Figure 6. Demonstrates the variation of the friction factor with the Reynolds numbers.

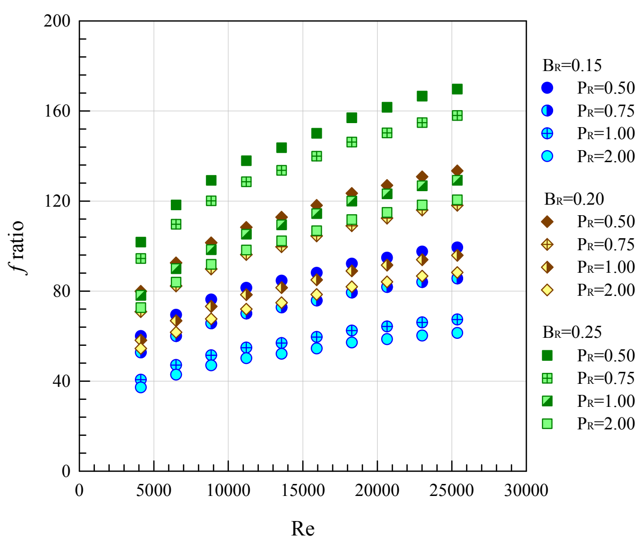

Figure 7. Demonstrates the variation of the friction factor ratio with the Reynolds numbers.

4.4 Effect of V-downstream winglet on thermal performance

Figure 8 shows the variation of the thermal performance (η) with Reynolds number (Re). For all, the data obtained by the measured Nu and *f* values are compared at the constant pumping power. It can be seen in the figure that the η generally are above unity for 45º V-downstream winglet inserted insert, indicating that the use of 45º V-downstream winglet turbulators is advantageous over the smooth duct. The η for using the 45º V-downstream winglet turbulators with P_R of 0.5, 0.75, 1 and 2 are approximately 1.60–1.92, 1.61–1.94, 1.64–1.97 and 1.52–1.82 times for B_R=0.15, 1.63–1.96, 1.66–1.99, 1.72–2.06 and 1.58–1.89 times for B_R=0.2 and 1.54–1.85, 1.55–1.87, 1.62–1.95 and 1.50–1.79 times for B_R=0.25. The mean *f* values for B_R=0.15, 0.2 and 0.25 are about 1.60–1.92, 1.63–1.96 and 1.54–1.85 times for P_R=0.5, 1.61–1.94, 1.66–1.99 and 1.55–1.87 times for P_R=0.75, 1.64–1.97, 1.72–2.06 and 1.62–1.95 times for P_R=1 and 1.52–1.82, 1.58–1.89 and 1.50–1.79 times for P_R=2 over the smooth duct. The maximum η of using 45º V-downstream winglet turbulators for B_R=0.15, 0.2 and 0.25 are 1.97, 2.06 and 1.95, respectively at Re=5300 and P_R=1 used in the present work.

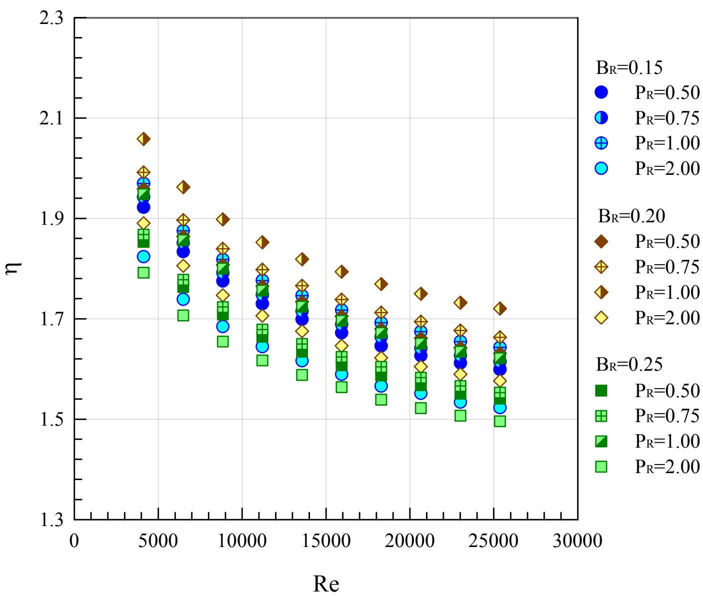

Figure 8. Demonstrates the variation of the thermal performance with the Reynolds numbers.

4.5 Empirical correlations

The empirical correlations for 45º V-downstream winglet turbulator developed by relating Reynolds number (Re), blockage ratio (B_R) and pitch ratio (P_R) from experimental data under the conditions; Re=4000–26,000, B_R=0.15–0.25 and P_R=0.5–2.0. The predicted Nusselt number and friction factor are, respectively, within ±7 and ±9 deviation with experimental results are shown in Figure 9 and 10, respectively.

Correlation of predicted Nu

$$Nu = 0.3242\,Re^{0.7916}\,Pr^{0.4}\,B_R^{\;0.3568}P_R^{\;0.1301} \quad (11)$$

Correlation of predicted f

$$f = 0.3242\,Re^{-0.0088}\,B_R^{\;1.2030}P_R^{\;-0.3056} \quad (12)$$

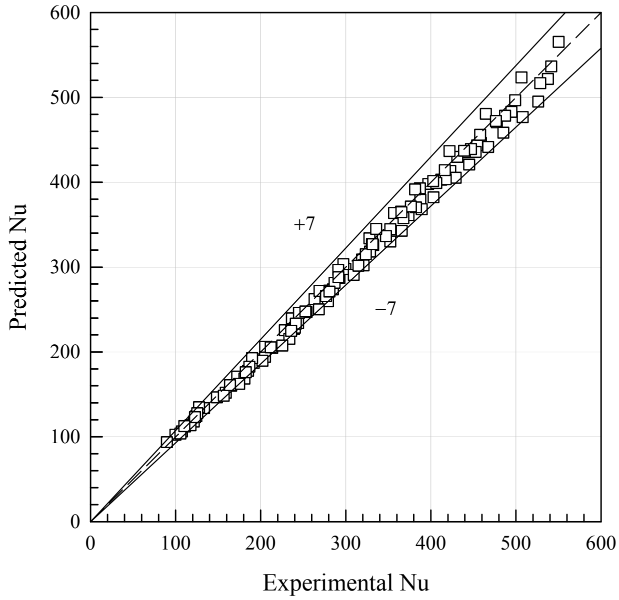

Figure 9. Variation tests of Nusselt number correlations.

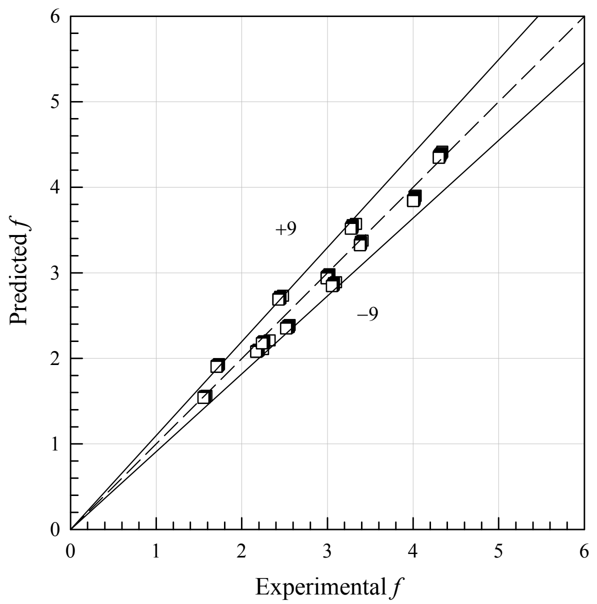

Figure 10. Variation tests of friction factor correlations.

5. Conclusion

An experimental study has been performed to investigate the heat transfer enhancement and thermal performance in a square-duct heat exchanger inserted with 45º V-downstream winglet turbulator with different pitch lengths and winglet heights for the turbulent regime, Re=4000–26,000 under uniform heat flux condition. From the experimental results of the present study can be conclude that the heat transfer rates and pressure loss are increased with the rise of the winglet heights and with the decreasing of the pitch lengths. The square-duct inserted with 45º V-downstream winglet is augmented the mean heat transfer rate higher than the smooth tube around 6.0 to 8.7 times, depending upon operating conditions. The maximum thermal performance for using 45º V-downstream winglet turbulator under the present experimental conditions is 2.06 at Re=4100, BR=0.2 and PR=1.0 in this experiment.

6. Acknowledgement

The authors would like to gratefully acknowledge the Thailand Research Fund (TRF) and Faculty of Industry and Technology, Rajamangala University of Technology Isan Sakonnakhon Campus.

7. References

(1) Hans VS, Saini RP, Saini JS. Performance of artificially roughened solar air heaters a review. Renewable and Sustainable Energy Reviews. 2009;13: 1854–1869.

(2) Mohsen Sheikholeslami, Mofid Gorji-Bandpy, Davood Domiri Ganji. Review of heat transfer enhancement methods: Focus on passive methods using swirl flow devices. Renewable and Sustainable Energy Reviews. 2015;49: 444–469.

(3) Varun, Saini RP, Singal SK. Investigation of thermal performance of solar air heater having roughness elements as a combination of inclined and transverse ribs on the absorber plate. Renewable Energy. 2008;33(6): 1398–1405.

(4) Zhou G, Ye Q. Experimental investigations of thermal and flow characteristics of curved trapezoidal winglet type vortex generators. Applied Thermal Engineering. 2012;37: 241–248.

(5) Promvonge P, Khanoknaiyakarn C, Kwankaomeng S, C. Thianpong C. Thermal behavior in solar air heater channel fitted with combined rib and delta-winglet. International Communications in Heat and Mass Transfer. 2011;38: 749–756.

(6) Won SY, Ligrani PM. Comparisons of flow structure and local Nusselt numbers in channels with parallel- and crossed-rib turbulators. International Journal of Heat and Mass Transfer. 2004;47: 1573–1586.

(7) Promvonge P, Jedsadaratanachai W, Kwankaomeng S. Numerical study of laminar flow and heat transfer in square channel with 30° inline angled baffle turbulators. Applied Thermal Engineering. 2010;30: 1292–1303.
(8) Promvonge P, Sripattanapipat S, Kwankaomeng S. Laminar periodic flow and heat transfer in square channel with 45° inline baffles on two opposite walls. International Journal of Thermal Sciences. 2010;49: 963–975.
(9) Chokphoemphun S, Chompookham T, Promvonge P. Heat transfer enhancement in a tube heat exchanger with a V-shape winglet turbulator. KKU Research Journal. 2014;19(2): 333–343.
(10) Chokphoemphun S, Pimsarn M, Thianpong C, Promvonge P. Heat transfer augmentation in a circular tube with winglet vortex generators. Chinese Journal of Chemical Engineering. 2015;23: 605–614.
(11) Cengel YA. Heat Transfer: A Practical Approach. 2nd ed. New York: Mc Graw-Hill; 2003.
(12) White FM. Fluid Mechanics. 4th ed. New York: Mc Graw-Hill; 1999.
(13) Webb RL. Principles of Enhanced Heat Transfer. New York: John-Wiley & Sons; 1992.
(14) ASME. Standard measurement of fluid flow in pipes using orifice, nozzle and venture. ASME MFC-3M1984 United Engineering Center 345 East 47th Street. New York: 1-56 1984.
(15) ANSI/ASME. Measurement uncertainty. 1986 PTC 19, Part I, 1-1985 1986
(16) Incropera FP, Witt PD, Bergman TL, Lavine AS. Fundamentals of heat and mass transfer. John-Wiley & Sons; 2006.